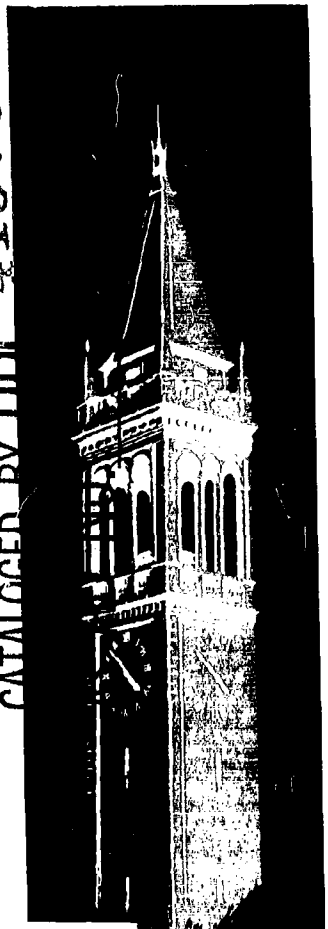

ASD-TDR-63-587

Electron Microprobe Developments For Integrated Circuit Research

by

T. E. Everhart

Series No. 60, Issue No. 461
Contract No. AF 33(616)-7553
October 22, 1962

ELECTRONICS RESEARCH LABORATORY
UNIVERSITY OF CALIFORNIA
BERKELEY, CALIFORNIA

ASD TECHNICAL DOCUMENTARY REPORT 63-587

Electronics Research Laboratory
University of California
Berkeley, California

ELECTRON MICROPROBE DEVELOPMENTS FOR INTEGRATED CIRCUIT RESEARCH

by

T. E. Everhart

Institute of Engineering Research
Series No. 60, Issue No. 461

Electronic Technology Division

Contract No. AF 33(616)-7553
Project No. 4159
Task No. 415906

Aeronautical Systems Division
Air Force Systems Command
United States Air Force
Wright-Patterson Air Force Base, Ohio

October 22, 1962

FOREWORD

This report was prepared by T. E. Everhart, of the University of California, Berkeley, California, on Air Force Contract No. AF 33(616)-7553, under Task No. 415906 of Project No. 4159, "Molecular Electronics." The work was administered under the direction of the Electronic Technology Division (formerly Electronic Technology Laboratory), AF Avionics Laboratory, Aeronautical Systems Division. Mr. Gordon Rabanus was Task Engineer for the Laboratory.

This is an interim report.

ABSTRACT

Analytic examination of semiconductor surfaces is possible using electron beams with diameters between 100 Å to 10,000 Å. Previous electron microprobe work in this field is reviewed; promising analytic methods for the future and fundamental limitations in the formation of electron microprobes are discussed. This work, which stresses analysis of semiconductor (or thin film) surfaces, thus complements the reports of Shoulders (1960) and Wells (1961), who stress fabrication of active circuits using electron-beam techniques.

TABLE OF CONTENTS

LIST OF ILLUSTRATIONS

I. INTRODUCTION

Giant advances in semiconductor technology over the past decade have made possible the present-day development of integrated circuits. These circuits are lightweight, compact and reliable, and are ideally suited to the requirements of space exploration. As their technology becomes better developed, and their fabrication yields increase, they will find important commercial applications for the above reasons and because of their lower cost/unit compared to conventional circuits fabricated from individual components. Hybrid circuits combining small dimensioned semiconductor and thin-film components on a single substrate also show great promise, including somewhat greater flexibility than is possible with circuits made using only semiconductor technology.

Integrated circuits are normally fabricated by the same methods as high-frequency planar transistors. Impurities are introduced into the semiconductor wafer by gaseous diffusion; the wafer surface is masked by an oxide layer, and impurities are able to diffuse into the wafer only where this oxide has been removed. The masking process is normally accomplished by photo-resist techniques, which have a resolution of approximately one micron. The resists are exposed with visible light using extremely high quality optical systems capable of resolving from 500 to 1000 lines/mm (a resolution of from one to two microns). In the production of integrated circuits, several successive resist exposures, oxide removal, and gaseous diffusion steps are necessary, and the registration of successive patterns on the semiconductor surface must be within one to two microns also if the ultimate device performance is to be realized. It is often difficult to determine during the device fabrication process whether or not this precise registration is being obtained at each step of the process. As semiconductor integrated hybrid devices become smaller, it also becomes more difficult to determine how closely the integrated circuit which is manufactured compares with the model which was designed for manufacture; best device performance is often achieved by empirical methods not completely understood by the design engineer.

Manuscript released by the author October 1962, for publication as an ASD Technical Documentary Report.

Mechanical probing to determine voltage changes along the semiconductor surface is a coarse method at these small dimensions. Light microscopy can yield details on surface structure and topography, but it does not yield quantitative electrical information.

II. SEMICONDUCTOR SURFACE EXAMINATION USING ELECTRON BEAMS

It would be desirable to examine integrated circuits with a high-resolution instrument which provides information on both the electrical and physical topography of the device surface. The examination should be non-destructive if possible so that it can be used as a quality-control step. Such examination is possible using very small diameter electron beams often called electron microprobes. An electron microprobe is produced by demagnifying a small electron source, using suitably placed electron lenses, and may have a typical diameter of a few microns to a few hundred angstrom units. For the semiconductor work of interest here, a beam ranging in diameter from 100 Å to 10,000 Å would be produced and scanned in a raster pattern over the semiconductor surface. The secondary emission of the semiconductor surface is a function of the surface geometry, and the number of secondary electrons which are collected is a function of the surface potential [Everhart, Wells and Oatley (1959)]. Thus if the collected secondary electron current is amplified, and the resulting video signal modulates the current of a cathode-ray tube which is scanned in synchronism with the electron microprobe, the picture appearing on the cathode-ray tube screen contains easily interpreted information on the physical and surface topography of the semiconductor specimen's surface. Such a scanning electron micrograph is shown as Fig. 1. This germanium pn diode was fabricated by alloying an indium pellet onto a germanium single crystal which had been ground, lapped and etched to a mirror flat surface along the (111) plane. The reverse-biased junction is seen in the micrograph as the sharp change of brightness, the light side to the right being the p region, and the darker side to the left being the n-type

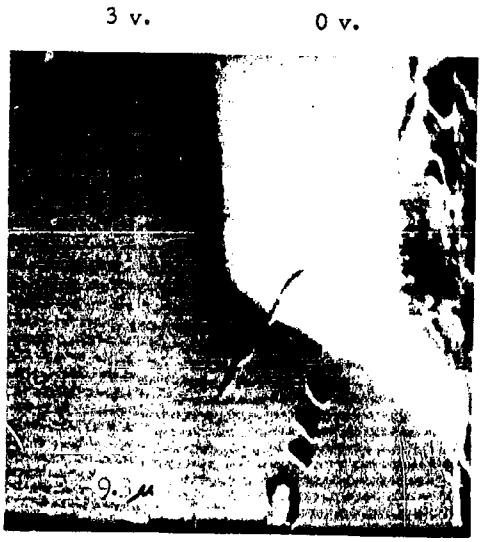

M = 1400

Fig. 1. Scanning Electron Micrograph of Germanium pn Junction with Reverse Bias of 3 Volts.

germanium. This low magnification micrograph also illustrates topographical contrast such as the holes and cracks in the specimen surface. The specimen is viewed at an angle; the ellipse shown in the lower left-hand corner represents a circle on the specimen surface.

It is worthwhile stressing that this is a nondestructive technique. For best resolution, scanning electron microscopes operate with beam voltages of 10-20 kV, and currents of the order of 10^{-8} to 10^{-12} amperes. The beam is scanned, i. e., is continually moving across the specimen surface, yielding an average power density at the specimen surface of considerably less than one milliwatt/square centimeter, and consequently, little heating of the specimen. The above voltage is much lower than that which produces structural damage such as Frenkel defects (lattice vacancy plus interstitial atom) in semiconductors; the threshold voltage for such defects is about 145 kV for silicon and above 325 kV for germanium [Loferski and Rappaport (1955)]. Damage may come from undesirable gaseous molecules in the vacuum system, which may condense on the surface and be polymerized by the electron beam. This contamination is discussed in more detail below; it does not seem a serious obstacle at the present time.

III. QUANTITATIVE MEASUREMENTS USING ELECTRON BEAMS

One inherent aspect of this technique is the electron beam which, in striking the specimen surface, injects carriers into the specimen to a depth of a few microns. (The actual depth depends both on material and beam energy). On insulating specimens, this charge causes electric fields, which spoil the resolution. On semiconducting and conducting specimens, this charge has no such bad effects. In fact, when high energy particles strike and penetrate into a semiconductor, they generate hole-electron pairs in the material. In silicon, for example, one hole-electron pair is generated for approximately each 3. 6 electron volts of energy of the incoming particle. For an impinging beam of current I at 3. 6 kV, a

current of 1000 I would flow if all these carriers could be utilized. Generally the minority carriers quickly recombine in the material, and these carriers are not utilized as current. However, if the hole-electron pairs are formed in a space charge or depletion region near the junction of a pn junction diode, the carriers are swept out of the junction region into the majority carrier region, and essentially all carriers which are created contribute to the current across the junction. Thus for a 20 kV electron into the depletion layer of a silicon pn junction some 5,500 electrons or holes will be swept into the majority region, giving a current amplification in this case of 5,500. Because the time response of this current amplification is quite fast, being in the order of a few nanoseconds, this process is receiving considerable attention, not only for nuclear detectors [see Williams and Webb (1962)], but also for fast switching as applied to computers [see Brown (1961)].

This process should be quite valuable in the analysis of very small dimensioned integrated circuits. Consider the case of a simple pn junction diode which extends to the surface of the material and which is reverse-biased. As a very small diameter electron beam probe is swept across the surface of the diode perpendicular to the junction, it generates hole-electron pairs in the semiconductor material. These hole-electron pairs will diffuse into the material, the diffusion length being easily calculated if the minority carrier lifetime and diffusion constant of the material are known. When the electron beam is far from the junction the current across the junction will be a normal leakage surface current of the diode plus the reverse bias current across the junction (it is assumed that the electron beam current is considerably less than these other mentioned currents). As the electron beam approaches the junction, some of the minority carriers will diffuse to the junction and be swept by the electric field which exists there into the opposite side of the junction where they are majority carriers and therefore have a much lower probability of recombination. Because of current continuity, the total current across the junction will be the same as the current through the external circuit. When the electron beam strikes the depletion layer, virtually all of the

hole-electron pairs will be swept out to their respective majority regions and the junction current will be several thousand times the incident beam current for 15-20 kV incident electron energies. This junction current may be measured, which permits a check on the efficiency of hole-current pair production by incident ionizing radiation. Preliminary experiments such as the one just described were performed by the author during his doctoral work at the University of Cambridge [Everhart (1958)].

Epitaxial growth is often employed to form pn junction beneath the surface of a semiconductor device, thus reducing surface effects. A nondestructive method of measuring both the mean junction depth and the uniformity of the junction depth beneath the semiconductor surface is of considerable interest. Electron-beam creation of hole-electron pairs which diffuse to the junction should be a nondestructive method of measuring the junction depth, provided the minority carrier's diffusion length in the material is known. The relative junction depth with position can be measured without knowing this diffusion length.

An important part of the planned work utilizing electron beams in this project involves starting with known pn junction diodes and correlating experimental and analytical calculations to determine exactly what happens when a very small diameter electron beam is swept across a pn junction which has a reverse bias across it. Once this is known, then the analysis will be extended to more complicated shapes and geometries, and again experimental and analytical calculations will be carefully correlated. The ultimate objective of this work will be the examination of any integrated circuit (which has leads attached so that external currents can be measured) and the direct or indirect determination of properties of its materials, such as doping, diffusion length, minority carrier lifetime, trap density, surface recombination velocity, etc. As semiconductor integrated circuits become smaller and more complex this may well be the only technique for determining what is happening "in the small". Knowledge provided in this way should be very valuable in the improvement of integrated circuits.

IV. ELECTRON MICROPROBE FORMATION

This interim report discusses the formation of an electron microprobe and the fundamental limitations on its performance. Many of these results are available in widely scattered literature; some results have been derived for presentation here.

For the analysis of integrated circuits discussed above, the scanning electron microscope [McMullan (1953), Smith and Oatley (1955), Everhart, et al., (1959)], seems the most promising instrument to use. A schematic of such an instrument is shown in Fig. 2. The source is traditionally the crossover from a conventional electron microscope gun employing a tungsten hairpin filament. The first lens produces a de-magnified image of the crossover and the second lens further demagnifies the crossover. If the deflection coils are not excited, the demagnified image of the crossover appears at the center of the specimen as shown in the figure. If the deflection coils are excited the demagnified crossover is deflected across the surface of the specimen in any desired pattern; for the scanning electron microscope a regular raster pattern used in conventional television is generally employed. Lens one and lens two may either be electrostatic or electromagnetic lenses of the type used in conventional electron microscopes. The only special feature of lens two should be a maximum working distance (i.e., distance between the outside of the lens and the specimen), consistent with minimum focal length. Spots as small as 300 angstrom units in diameter have been produced by a scanning electron microscope at Cambridge University. Larger spots can, of course, be produced by increasing the focal length of either lens. In order to produce such a fine spot both the high voltage and the lens current power supplies must be extremely stable, and the mechanical rigidity of the instrument must also be extremely high.

Often it is desirable to pulse the current which strikes the specimen surface. If the power supply is pulsed, variation in the power supply voltage can occur which seriously impairs the resolution of the instrument. For this reason the usual method of pulsing the current at the specimen is to deflect the beam off the final aperture by the beam blanking deflection coil shown in Fig. 2. A fast rise time pulse applied to this coil will

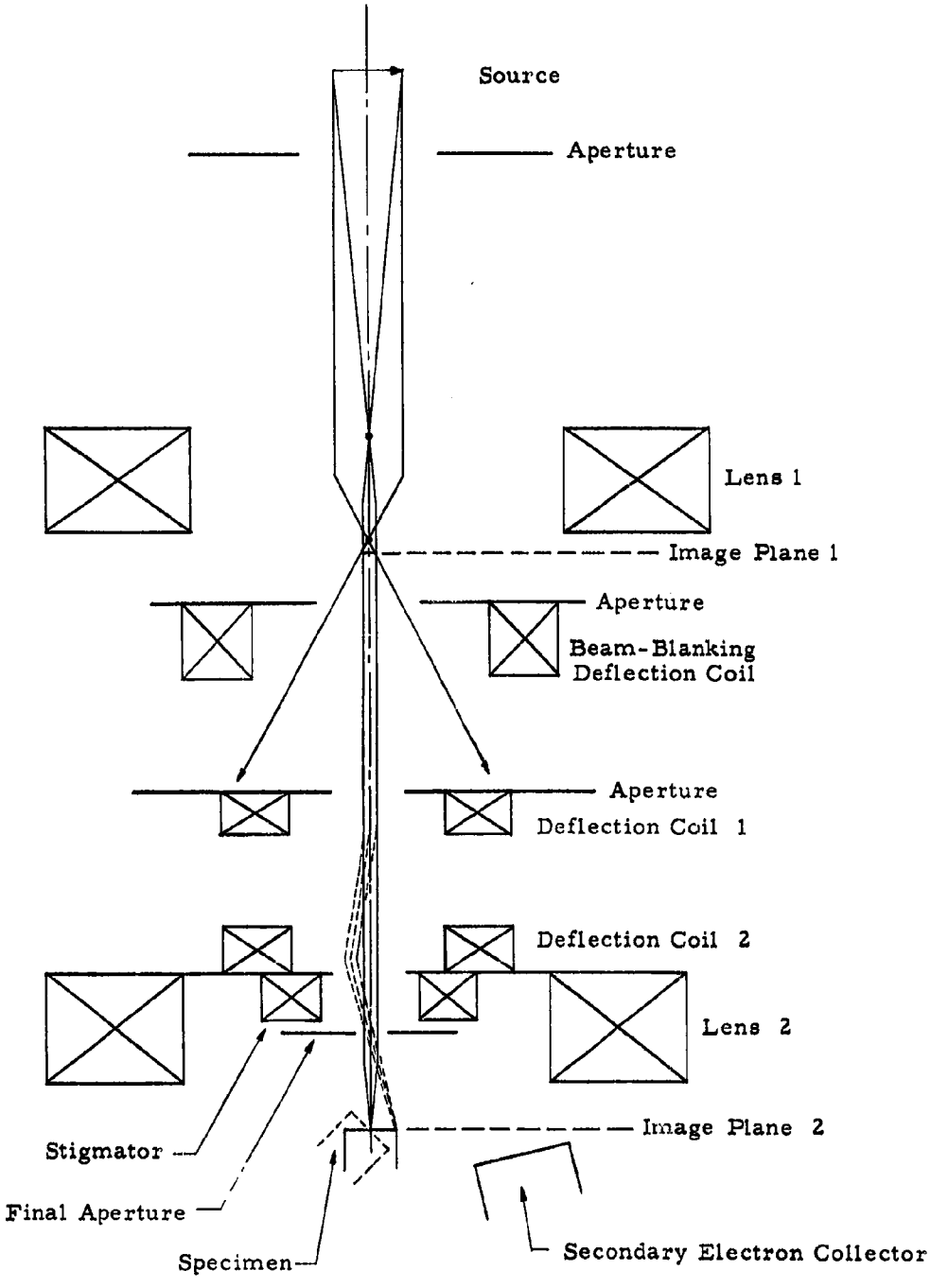

Fig. 2. Simplified schematic diagram of scanning electron microscope column

deflect the beam from the specimen; essentially no current strikes the specimen while the pulse is on, and full current strikes the appropriate part of the specimen when the coil is not excited. (Electrostatic deflection plates would serve this purpose equally well).

Two deflection coils for each dimension of deflection precede the final lens in the scanning electron microscope, whereas in a cathode ray tube only one deflection coil/dimension is used, and it follows the focusing lens. If the lens follows the deflection coils, it can be much closer to the specimen surface and therefore a much greater demagnification of the spot can occur. Also the spot appears virtually at the focus of the lens, which minimizes the effect of spherical aberration. Two deflection coils are generally used in order that the deflected and undeflected beam axes may coincide at the center of the final lens where the final aperture is located. This gives the maximum current density at the specimen and also the largest deflection area without vignetting.

Although the physical arrangement of deflection coils and final lens that is shown in Fig. 2 are normal for scanning electron microscopes, the desire to scan an electron beam of very small diameter over many spot diameters may require that the electron lens precede the deflection coils as in the microfocus cathode ray tube described by Schlessinger (1961) in which an eight micron spot with a beam current of 1.5 microamperes is deflected over a five inch cathode ray tube face with a resolution of ten thousand lines. While such a geometry does not seem feasible at the much smaller spot sizes desired in the scanning microscope, nevertheless an investigation is under way to determine the optimum geometry for a given spot size and number of spot-diameters to be deflected.

V. FUNDAMENTAL LIMITATIONS

The performance of electron optical apparatus is limited by certain fundamental limitations. There is a certain practical maximum current density which can be drawn from a thermionic cathode, and this limits the current density throughout the apparatus. The statistical nature of

thermionic emission causes a fundamental shot noise, and the Maxwellian velocity distribution of thermionic electrons places a further restriction on the maximum current density in the image plane. Axially-symmetric electron lenses have an inherent spherical aberration which can be minimized through proper design, but cannot be eliminated. They also possess an inherent astigmatism due to imperfections in manufacture (tolerances may be a few millionths of an inch!) and to inhomogeneities in the magnetic material (for magnetic lenses only). At a given lens strength, the astigmatism may be corrected electrically; thus it is not a fundamental limitation, although it may be troublesome if lens strength is varied often. At very small spot sizes or at low voltages the wavelength of the electron may limit the spot size due to diffraction effects. The resolution which is obtained may be limited by scattering of electrons in the specimen material, and a material being processed or examined by an electron probe may be altered or contaminated by the beam itself, or by the beam in conjunction with gaseous molecules present in demountable vacuum systems.

A. Cathode Current Density

One of the best electron emitters for demountable vacuum systems is tungsten heated to from 2700 to 3000° K. The current density is a rather sensitive function of temperature in this range of temperature, approximately doubling for each 100° increase in cathode temperature. While tungsten must be heated to a higher temperature than many other metals, it has proven quite satisfactory, and is used in most electron-optical demountable systems. The specific emission of tungsten varies from approximately 1.5 amps/sq. cm. at 2700° K to approximately 10 amps/sq. cm. at 3000° K. The choice of operating temperature depends on the desired life-time of the emitter as tungsten evaporates more rapidly at the higher temperatures. Operation at temperatures exceeding 3000° K results in very short filament life-time.

Other thermionic emitters which are sometimes used in demountable systems are thoriated tungsten cathodes, oxide cathodes, and impregnated cathodes. The latter two are quite susceptible to poisoning unless extreme precautions are taken, but have the advantage of a somewhat lower

operating temperature.

Impregnated cathodes activate rapidly, and appear attractive for use in "clean" systems, where the pressure is maintained below 10^{-6} Torr. Such systems may prove advisable to avoid surface contamination of semiconductor specimens due to hydrocarbon molecules from diffusion pump oil and O-ring seals. Some advantages and disadvantages of "clean" systems are discussed under the heading of Contamination.

Another promising electron source for microprobe applications is a field emitter cathode. At the present time these cathodes require a very low pressure of the order of 10^{-9} millimeters of mercury or less. Quite large current densities are obtained from the emitter tip, but the tip itself is quite small, and so the total emitted current is generally quite small. Cosslett and Haine (1954) have shown the field emitter cathode superior to the ordinary thermionic cathode if the spot produced is of the order of a few hundred angstrom units or less. Recent encouraging work on a new geometry of field emitter cathode [Shoulders (private communication)] may make the field emitter cathode more competitive with thermionic cathodes at the larger spot diameters as well, but the need for very low pressures in order to ensure stable operation persists.

The work reported on in the balance of this report will assume a tungsten thermionic cathode with the understanding that when better cathodes of a different type become available, they certainly will be exploited.

B. Noise

The statistical fluctuation of the number of electrons emitted per unit time in thermionic emission is termed shot noise and has been analyzed by many workers in some detail. Noise as it applies to the scanning electron microscope has been adequately discussed by Smith and Oatley (1955) and Everhart, Wells and Oatley (1959), and is only briefly reviewed here. Basically, the noise per picture point in a scanned display is due to the shot noise in the primary electron beam, plus any additional noise due to secondary emission from the specimen under examination, and noise introduced by subsequent amplification. The mean-square noise current is

proportional to average beam current and bandwidth; the mean-square signal current is proportional to average beam current squared; thus the signal-to-noise ratio increases with beam current and decreases with increased bandwidth. For this reason, the video bandwidth must be greatly reduced at the small beam currents used in a scanning microscope (from 10^{-8} to 10^{-12} amperes).

C. Axial Current Density

The maximum current density which can be obtained in an axially symmetric system with no aberrations was first derived by Langmuir (1937). This maximum current density is

$$J_m = J_c \left[1 + \frac{eV}{kT}\right] \sin^2 \alpha \doteq J_c \frac{eV}{kT} \alpha^2 \qquad (1)$$

where J_c is the cathode current density, V is the accelerating voltage between the cathode and the point in question, T is the temperature in degrees Kelvin, α is the half-angle of convergence of the electron beam at the point in question, e is the electronic charge and k is Boltzmann's constant. Equation (1) was derived assuming only that the electrons are emitted with a Maxwellian velocity distribution, and that the electron optical system obeys Abbe's sine condition.

D. Spherical Aberration

It is well known that electron lenses possess a finite spherical aberration coefficient. Spherical aberration is the only fundamental electron optical aberration which does not vanish on the axis. If a perfectly parallel beam of electrons is incident on an axially symmetric electron lens from the left, it is imaged on the right to a disc of confusion slightly in front of the focal plane with a diameter d_s given by the following equation:

$$d_s = 0.25\, C_s \alpha^3 \qquad (2)$$

If the electrons are diverging from an object to the left of the lens, the

disc of confusion is imaged slightly in front of the normal image plane and has a diameter given by Eq. (2) with C_s replaced by C'_s where

$$C'_s = C_s \left(\frac{b}{f}\right)^4 \tag{3}$$

In this equation, b is the distance from the lens to the image plane, f is the focal length of the lens and C_s is the spherical aberration constant given by graphs in most of the standard books on electron optics, for example, in Zworykin, et al. (1945). Equation (3) is essentially given by von Ardenne (1956, table 15).

E. Limiting Spot Size

It is often desirable to know the limiting spot size obtainable with a given electron optical system. It will be assumed here that this minimum spot size is limited by the Gaussian spot size, by spherical aberrations, and by thermionic emission velocities. The Gaussian spot size is determined from the object size, generally taken as a crossover formed by the electron gun, and by the demagnification as determined by the geometry of the electron lenses. The effect of thermal velocities will be taken as the approximate form of Eq. (1) since (eV/kT) is generally much greater than unity in electron optical systems of interest and α is generally much less than unity. As we shall be interested in demagnified images, b/f will be taken as unity, although any result we obtain can be adjusted to b/f different from unity, but substituting C'_s for C_s. The crossover of an electron gun has a Gaussian variation with radius, and the current density in the minimum disc of confusion due to spherical aberration has a similar bell-shaped variation with radius. Thus to get the total spot diameter the Gaussian spot diameter and the spherical aberration spot diameter should be added in quadrature.

$$d^2 = d_g^2 + d_s^2 \tag{4}$$

where d is the total spot diameter, d_g is the Gaussian spot diameter,

and d_s has been defined in Eq. (2) above. The current in the Gaussian spot may be found from the approximate form of Eq. (1) if the crossover is demagnified sufficiently.

$$I = \frac{\pi}{4} d_g^2 J_c \frac{eV}{kT} \alpha^2 \tag{5}$$

If Eq. (2) and Eq. (5) are substituted into Eq. (4), the spot diameter d may be written as

$$d = \left\{ \left[\frac{4 I k T}{3\pi J_c e V} \right]^{3/4} \frac{3}{2} C_s^{1/2} \left[\left(\frac{\alpha_o}{\alpha} \right)^2 + \frac{1}{3} \left(\frac{\alpha}{\alpha_o} \right)^6 \right] \right\}^{1/2} \tag{6}$$

In the last equation, an optimum value of the beam convergence angle α has been used. This optimum value is the value which gives the minimum spot diameter for a specified current I at the spot, current density at the cathode J_c, cathode temperature T, accelerating voltage V, and spherical lens aberration coefficient C_s. This optimum value of α is found by usual minimization techniques and is given as

$$\alpha_o = \left[\frac{64 I k T}{3\pi C_s^2 J_c e V} \right]^{1/8} = \frac{0.394}{C_s^{1/4}} \left[\frac{IT}{J_c V} \right]^{1/8} \tag{7}$$

The optimum diameter for a given value of the various parameters is given by

$$d_o = \left[\frac{4 I k T}{3\pi J_c e V} \right]^{3/8} 2^{1/2} C_s^{1/4} \tag{8}$$

The current I which occurs in Eq. (8) is the maximum current which can be focused into a demagnified spot of diameter d_o by an axially-symmetric electron-optical system. Solving Eq. (8), this optimum current is obtained.

$$I_o = \frac{3\pi 2^{2/3}}{16} J_c \frac{eV}{kT} \frac{d_o^{8/3}}{C_s^{2/3}} = 10,900 \frac{J_c V}{T C_s^{2/3}} d_o^{8/3} \tag{9}$$

For design purposes, it is important to know not only the optimum value of a given dependent variable as a function of the independent variable, but also the variation about this optimum value. For example, it is interesting to plot the variation of the current as a function of the beam aperture angle α for constant values of J_c, V, T, the spherical aberration coefficient C_s and the total spot diameter d. The analytic expression for the current is

$$I = \frac{\pi}{4} J_c \frac{eV}{kT} d^2 \alpha^2 \left[1 - \left(\frac{\alpha}{\alpha_m}\right)^6\right] \tag{10}$$

where α_m is the α for which the total spot diameter is due to spherical aberration and none due to the Gaussian spot. Therefore the current must vanish at $\alpha = \alpha_m$.

$$\alpha_m = \left[\frac{4d}{C_s}\right]^{1/3} \tag{11}$$

The pertinent graph is shown in Fig. 3. As α increases from zero, the current increases quadratically since the effect of spherical aberration is exceedingly small. At the optimum value of α the current reaches its maximum and then rapidly decreases as α increases further because in order to maintain a spot of constant diameter, the Gaussian spot size must be rapidly reduced to compensate for the rapid increase of aberration spot size.

Another important design curve is the plot of normalized spot diameter d versus normalized α for a constant spot current. This plot (Fig. 4) assumes that the cathode current density, absolute temperature, beam voltage, and spherical aberration coefficient are all held constant,

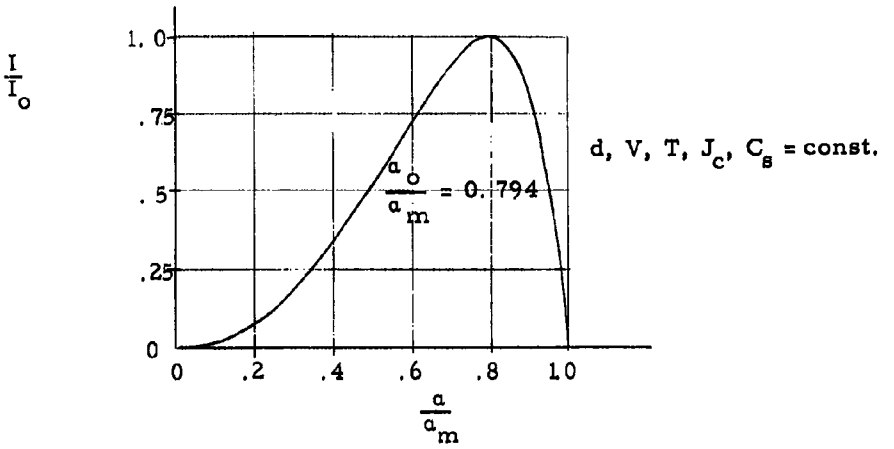

Fig. 3 Beam Current vs. Convergence Angle for a Fixed Spot Diameter

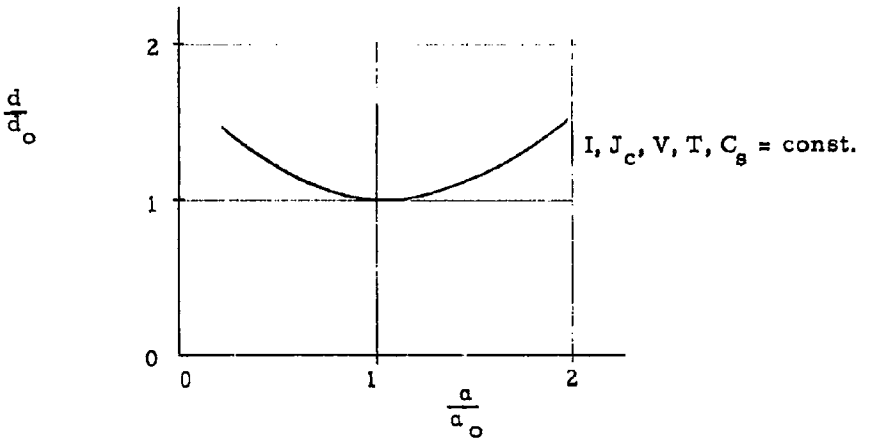

Fig. 4 Spot Diameter vs. Convergence Angle for a Fixed Beam Current

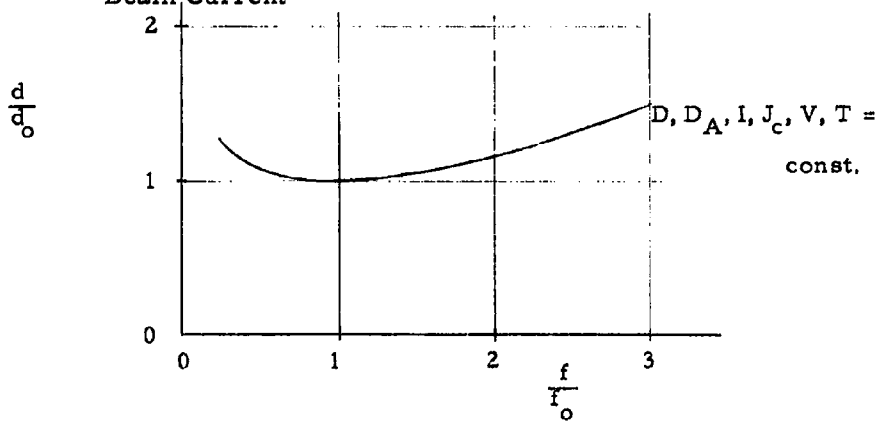

Fig. 6 Spot Diameter vs. Focal Length for Fixed Final Aperture Diameter and Beam Current (Typical Operating Conditions)

and shows that the spot diameter is not a rapidly varying function of the beam convergence angle α. For design purposes this implies that if a given value of spot diameter d_o were selected, and then α was somewhat different than the design value α_o, the resulting true spot diameter d would not greatly exceed the design value.

Another important design question is "How does the spot diameter vary as the focal length of the final lens is varied in order to focus the beam onto a target surface at greater or lesser distance from the lens?" To answer this question, the variation of the spherical aberration coefficient with the lens focal length must be known. While there are no analytic expressions for this parameter as a function of focal length, from calculations and measurements given by Zworykin, et al., (1945, p. 614, Fig. 17. 7), and Liebmann and Grad, (1951, Fig. 21), an empirical value of the spherical aberration coefficient as a function of the lens bore diameter, D, and the lens focal length f, may be written as

$$C_s = 2D^{-7/4} f^{11/4} \tag{12}$$

where C_s, f and D are in centimeters. The beam convergence angle α is a function of the focal length also and of the diameter of the final aperture D_A; the relationship is easily found from Fig. 5 to be

$$\alpha = \frac{D_A}{2f} \tag{13}$$

when the values of C_s and α given by the preceding two equations are substituted into Eq. (6), the following value for d/d_o results.

$$\frac{d}{d_o} = \left[\frac{1}{5} \left(\frac{f}{f_o} \right)^2 + \frac{4}{5} \left(\frac{f}{f_o} \right)^{-1/2} \right]^{1/2} \tag{14}$$

where the optimum value of the focal length is given by

$$f_o = \frac{D^{-7/5} D_A^{16/5}}{64} \left[\frac{2\pi J_c eV}{IkT} \right]^{2/5} = 1.38 D^{-7/5} D_A^{16/5} \left[\frac{J_c V}{IT} \right]^{2/5} \tag{15}$$

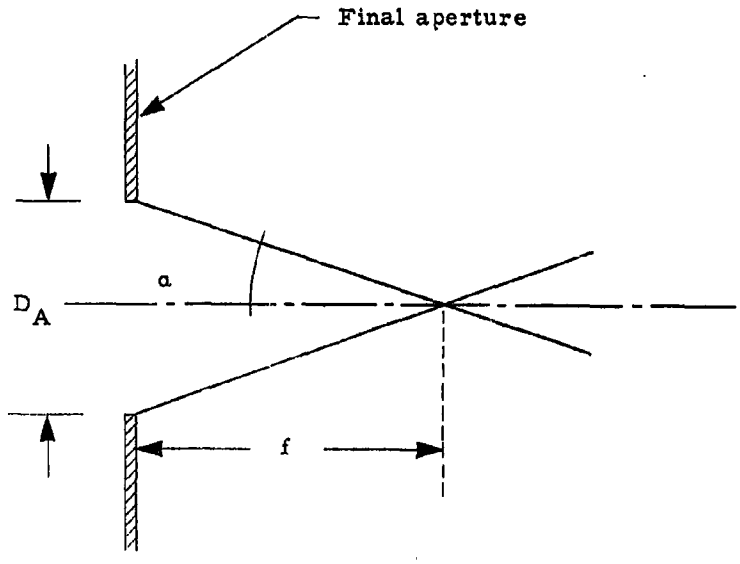

Fig. 5 Sketch Showing the Geometrical Relationship between α, D_A, and f

As can be seen from Fig. 6, the spot diameter does not increase rapidly over the optimum spot diameter for large changes of the focal length. For example, if the focal length is doubled, the spot diameter increases about 35%.

The equations and graphs of this section aid the design of a microprobe and indicate the performance which may be expected. Equation (12) shows that C_s is minimized by using the shortest possible focal length f and largest lens diameter D. However, if D is too large, the magnetic material of which the lens is constructed will saturate; also, the minimum focal length of a magnetic lens is proportional to its diameter. Hence, lens design always involves compromises; using procedures and curves

due primarily to Liebmann (1955) and Mulvey (1958), electron-probe magnetic lens design is fairly readily accomplished.

F. Resolution

Resolution has been discussed in some detail by Everhart et al. (1959). For thick targets, resolution is a function of electron scatter by the target material, as well as of the electron spot size. Although the primary electrons may be scattered over a volume of target material which extends to a depth R into the target (where R is the range in the target material), most secondaries excited directly by the primary beam are estimated to escape from within about 100 Å of the point of entry of the primary electrons. Some secondary electrons are excited by back-scattered electrons, i.e., those primary electrons which have suffered a large-angle deflection, and escape the target with a sizable fraction of the primary energy. These electrons (and the secondaries they excite) generally leave the target within a distance of approximately R/3 of the primary electron's entry point. For very high resolution work they present a background noise which degrades the signal. For lower resolution work, where the resolution desired is less than R/3, they contribute a useful video signal. Thus the resolution possible with a scanning electron microscope is believed to be approximately 100 Å or better (300 Å has been achieved experimentally, and performance was not limited by fundamental considerations, but by electron spot size). These considerations of resolution hold whether contrast is caused by physical or voltage topography of the specimen surface.

A different criteria of "resolution" exists when the reverse-bias current through a pn junction as increased by the electron beam is being monitored. First the change in junction current must be detectable with certainty; this specifies a minimum beam current at a given beam voltage. This beam current and voltage specifies a minimum spot diameter d; the diameter of the irradiated volume in the target will be increased over this spot diameter by scattering. If R is the maximum range of the primary electrons in the target material, then the mean diameter of the irradiated

volume may be approximated by d + R. Often the variation of energy dissipation with depth into the material is also important, as hole-electron pair production is directly proportional to energy dissipation. The energy dissipation/unit depth depends upon the primary electron energy and the target material to some extent, according to Kanter and Sternglass (1962) and Kanter (private communication), but a universal curve derived from range measurements in air is believed to be a good approximation for electron penetration of solids as well [Grün (1957)]. This universal curve shows the energy dissipation/unit depth rising from its value at the surface to a maximum at approximately 0.3 R, and then decreasing to zero at R. The value at 0.6 R is approximately the same as at the target surface.

The actual shape of the irradiated volume has been discussed by various authors, but no widely applicable measurements have been performed, primarily because of the difficulty of recording and interpretating quantitative data. (Some pictures by Ehrenberg and Franks (1953) showing florescence in insulators bombarded with an electron probe are indicative of the possible shape of the irradiated volume, but are suspect as to their detailed shape because of possible charging effects within the material.) For many analyses, the electron-irradiated volume can be approximated by a point source of hole-electron pairs. However, for examination of "hidden" junctions a few microns beneath the semiconductor surface, the energy dissipation/unit depth should be known more accurately, and for determining semiconductor parameters as the beam is swept over a junction at the semiconductor surface, the variation of energy dissipation with distance from the beam axis should be known accurately as well. Examination of an angle-lapped abrupt semiconductor pn junction may provide a method of measuring the energy dissipation/unit depth, and similar examination of an abrupt junction normal to the surface may yield the energy dissipation with distance from the beam axis. In both cases, the reverse-bias current through the junction would be measured accurately as the beam is swept over the specimen, and the shape of the reverse-bias current vs. beam position curve interpreted analytically to give the required information.

G. Contamination

In demountable vacuum systems pumped by oil vapor diffusion pumps, a layer or layers of hydrocarbon atoms can build up on surfaces on the interior of the vacuum system. If an energetic electron beam strikes these surfaces, these hydrocarbon atoms generally are cross-polymerized and an insulating film is formed on the surface. Christy (1960) has analyzed one model of this process quite carefully, both experimentally and theoretically. His theory shows that the rate of film formation is proportional to the number of molecules which strike the surface per unit area per unit time. This rate of film formation is decreased if the substrate temperature is increased or if the quality of the vacuum is greatly improved.

The above form of contamination has long been a problem in electron microscopy, where contamination can injure the specimen under examination and impair instrumental resolution. Heide (1962) has shown that if a specimen is kept at room temperature, but surrounded by a vessel at a temperature less than -130° C, (liquid nitrogen is excellent as a coolant), the rate of contamination is reduced by two or three orders of magnitude below the rate which occurs without these precautions (the operating pressure of electron microscopes is approximately 5×10^{-5} Torr). Reduced contamination occurs principally because hydrocarbons and water vapor molecules which enter the specimen chamber are condensed on the cold walls, but not on the warm specimen. The specimen chamber must be designed, therefore, with all surfaces except the specimen itself at liquid nitrogen temperature. If this procedure is followed, then ordinary demountable vacuum practice can be followed throughout the rest of the system, including the use of O-ring seals, brass and mild steel parts, etc.

Another method for reducing contamination is simply to operate an ultra-high vacuum system. Such a system would use low vapor pressure material, would be capable of bake-out, and would be processed like a sealed-off vacuum tube. It might use a dispenser-type cathode, with a much greater life than is normal with tungsten filaments, and with a lower operating temperature. It could be pumped with an ion-gettering pump, which introduces no hydrocarbons or other contaminating materials.

However, mechanical motions are far more difficult to introduce into such a vacuum system, and its fabrication and maintenance are also more difficult.

VI. CONCLUSIONS

A complex potential distribution on the surface of a semiconductor device, such as a transistor or integrated circuit, can be observed directly in the scanning electron microscope with resolution limited only the the electron beam spot diameter and scattering processes in the target material*. In addition, the electron beam itself serves as a source of hole-electron pairs which can be usefully employed in integrated circuit analysis. Certain promising applications of the scanning microscope for integrated circuit inspection and analysis have been discussed in a preliminary manner, and practical limitations of the instrument have been either described or referenced. The construction of a scanning microscope to exploit the above ideas is planned at the University of California, and certain components, such as the high-stability power supplies, have already been procured. The actual instrumental construction will start in June, 1963.

*Note added in proof: Recent experiments by the author at the Westinghouse Research Laboratories, Pittsburgh 35, Pennsylvania, have demonstrated that potential distributions can be observed on the surfaces of passivated integrated circuits, i.e., on semiconductor surfaces covered with a silicon dioxide layer several thousand Angstrom units thick.

REFERENCES

1. Brown, A. V., "A multi-position magnetic core driver using electron-beam switched p-n junctions", paper presented at the Electron Devices Conference, Washington, D. C., October 1961.
2. Christy, R. W., "Formation of thin polimer films by electron bombardment", J. Appl. Phys. 31, 1680-1683, September 1960.
3. Cosslett, V. E., and Haine, M. R., "A tungsten point cathode as an electron source", Proc. International Conference on Electron Microscopy, pp. 639-644, London, 1954.
4. Ehrenberg, W., and Franks, J., "The penetration of electrons into luminescent materials", Proc. Phys. Soc., B 64, 1057-1066, 1953.
5. Everhart, T. E., "Contrast formation in the scanning electron microscope," doctoral thesis, University of Cambridge, Cambridge, England, 1958.
6. Everhart, T. E., Wells, O. C., and Oatley, C. W., "Contrast and resolution in the scanning electron microscope", J. Electronics and Control, 7, 97-111, 1959.
7. Grün, A. E., "Lumineszenz-photometrische Messungen der Energie-absorption im Strahlungsfeld von Elektronenquellen Eindimensionaler Fall im Luft", Zeitschrift fur Naturforschung, 12a, 89-95, 1957.
8. Heide, H. G., "The prevention of contamination without beam damage to the specimen", Proc. Fifth International Congress for Electron Microscopy, Vol. I, A-4, Academic Press, 1962.
9. Kanter, H., and Sternglass, E. J., "Interpretation of range measurements for kilovolt electrons in solids", Phys. Rev. 126, 620-626, 1962.
10. Langmuir, D. B., "Theoretical limitations of cathode-ray tubes", Proc. IRE, 25, 977-991, 1937.
11. Liebmann, G., and Grad, E. M., "Imaging properties of a series of magnetic electron lenses", Proc. Phys. Soc., B 64, 956-971, 1951.
12. Liebmann, G., "The magnetic pinhole electron lens", Proc. Phys. Soc., B 68, 682-685, 1955.

13. Loferski, J. J., and Rappaport, P., "Thresholds for electron bombardment induced lattice displacements in silicon and germanium", Phys. Rev., 100, 1261, 1955.
14. McMullan, D., "An improved scanning electron microscope for opaque specimens", Proc. IEE, 100, pt II, 245-259, 1953.
15. Mulvey, T., "Electron-optical design of an X-ray micro-analyser", J. Sci. Instr., 36, 350-355, 1959.
16. Schlesinger, K., "A display for 100 Million dots on a 5-inch face", paper presented at the Electron Devices Conference, Washington, D. C., October 1961.
17. Shoulders, K. R., "Research in microelectronics using electron-beam activated machining techniques", Stanford Research Institute Interim Report on Contract NONR-2887(00), September 1960.
18. Smith, K. C. A., and Oatley, C. W., "The scanning electron microscope and its fields of application", Brit. J. Appl. Phys., 6, 391-399, 1955.
19. Steigerwald, K. H., "Electron beam milling", Proceedings of the Third Electron Beam Symposium, 269-290, Alloyd Electronics Corp., March 1961.
20. von Ardenne, M. "Tables of electron physics, ion physics, and electron microscopy", Veb Deutscher Verlag der Wissenschaften, Berlin, 1956 (English translation Astia Report 254520, 1960).
21. Wells, O. C., "Electron beams in micro-electronics", Proceedings of the Third Symposium on Electron Beam Processes, 291-321, Alloyd Electronics Corp., March 1961.
22. Williams, R. L. and Webb, P. P., "Silicon junction nuclear particle detectors", RCA Review, 23, 29-46, March 1962.
23. Zworykin, V. K., Morton, G. A., Ramberg, E. G., Hillier, J. and Vance, A. W., Electron Optics and the Electron Microscope, John Wiley and Sons, Inc., New York, 1945.

DISTRIBUTION LIST
Contract AF 33(616)-7553

ORGANIZATION	NO. COPIES
Commander Aeronautical Systems Division Wright-Patterson Air Force Base Ohio ATTN: ASRCA	1
Commander Aeronautical Systems Division Wright-Patterson Air Force Base Ohio ATTN: ASAD (RAND)	1
Commander Aeronautical Systems Division Wright-Patterson Air Force Base Ohio ATTN: ASAD (Library)	1
Commander Aeronautical Systems Division Wright-Patterson Air Force Base Ohio ATTN: ASAT	1
Commander Aeronautical Systems Division Wright-Patterson Air Force Base Ohio ATTN: ASRNEM-2	20
Commander Aeronautical Systems Division Wright-Patterson Air Force Base Ohio ATTN: ASRMC	1
Commander Aeronautical Systems Division Wright-Patterson Air Force Base Ohio ATTN: ASRE	1
Commander Aeronautical Systems Division Wright-Patterson Air Force Base Ohio ATTN: ASRMP	1
Commander Aeronautical Systems Division Wright-Patterson Air Force Base Ohio ATTN: RALA (LIBRARY)	1
Commander Aeronautical Systems Division Wright-Patterson Air Force Base Ohio ATTN: ASDSS	1
Commander Aeronautical Systems Division Wright-Patterson Air Force Base Ohio ATTN: MCLI (LIBRARY)	1
Air Force Systems Command ATTN: MCRRP Andrews Air Force Base Washington 25, D.C.	1
Air Force Systems Command ATTN: RDRESE, Mr. Presnell Andrews Air Force Base Washington 25, D.C.	1
United States Air Force Security Service ATTN: CLR San Antonio, Texas	1
Air Force Cambridge Research Laboratories ATTN: Documents Unit, CRDOTR-2 L. G. Hanscom Field Bedford, Massachusetts	1
Rome Air Development Center ATTN: RAWLD Griffiss Air Force Base Rome, New York	1
Rome Air Development Center ATTN: RCWDI, Michael P. Forin Griffiss Air Force Base Rome, New York	1
Air Force Development Field Representative ATTN: Code 1072 Naval Research Laboratory Washington 25, D.C.	1
Air Force Missile Test Center Patrick Air Force Base Florida	1
Air Force Office of Scientific Research ATTN: C. Yost Washington 25, D.C.	1
Air Force Office of Scientific Research ATTN: D. L. Mannerstan Washington 25, D.C.	1
Air Force Special Weapons Center ATTN: SWOI Kirtland Air Force Base New Mexico	1
Air Force Systems Command ATTN: RDLDT, Captain Zimmerman Andrews Air Force Base Washington 25, D.C.	1

ORGANIZATION	NO. COPIES
Radio Corporation of America ATTN: Defense Electronic Products 75 Varick Street New York 13, New York	1
Ramo-Wooldridge, A Division of Thompson Ramo-Wooldridge, Inc. 8433 Fallbrook Avenue ATTN: Technical Information Services Canoga Park, California	1
Air University Library ATTN: 7575 Maxwell Air Force Base Alabama	1
AFSC Liaison Office Los Angeles Area ATTN: Major James L. Billie 6331 Hollywood Boulevard Hollywood 28, California	1
Headquarters, USAF ATTN: Mr. H. Mulkey Pentagon Washington, D.C.	1
Headquarters, USAF ATTN: WNSAL, Captain Stephenson Air Force Unit Post Office Los Angeles 45, California	1
Air Force Systems Command Office 346 Broadway New York 13, New York	1
Air Force Academy Palmer Lake, Colorado	1
School of Aviation Medicine USAF Aerospace Medical Center, ATC ATTN: SAMRSON Brooks Air Force Base Texas	1
AFSC Liaison Office San Francisco Bay Area 1176 Los Altos Avenue Los Altos, California	1
Commanding General U.S. Army Signal Research and Development Laboratories ATTN: Technical Documents Center Evans Signal Lab Area, Bldg. #27 Fort Monmouth, New Jersey	1
Commander Army Ballistic Missile Agency ATTN: ORDAB-DGC Redstone Arsenal, Alabama	1
Office of the Chief Signal Officer ATTN: SIGRD-4a Department of the Army Washington 25, D.C.	1
Commanding General U.S. Army Signal Research and Development Laboratories ATTN: SIGFM/EL-PE, Mr. A. W. Rogers Fort Monmouth, N.. Jersey	1
Commanding Officer U.S. Army Signal Equipment Support Agency ATTN: SIGFM/ES-MM-3, Mr. R. P. Iannarone Fort Monmouth, New Jersey	1
Commanding Officer U.S. Army Signal Equipment Support Agency ATTN: Technical Library ORDSR-OOTL Redstone Arsenal, Alabama	1
Commanding Officer U.S. Army Signal Electronic Research Unit ATTN: SIGRU-3, Major J. Adornetto P. O. Box 205 Mountain View, California	1
Chief, Bureau of Ships 691B, Electronics Division Room 3347, Main Navy Building ATTN: Mr. Edwin Hrug Washington 25, D.C.	1
Chief, Bureau of Weapons Avionics Division Material Coordination Unit Department of the Navy Washington 25, D.C.	1
Chief, Bureau of Ships ATTN: Code 817 Department of the Navy Washington 25, D.C.	1
Chief, Bureau of Weapons ATTN: Mr. J. M. Lee Department of the Navy Washington 25, D.C.	1
Commander Department of the Navy U.S. Naval Avionics Facility ATTN: Mr. Carl Ferguson Indianapolis 18, Indiana	1
Commanding Officer U.S. Army Signal Research and Development Laboratory ATTN: SIGFM/EL-PEC Mr. R. A. Garhold Fort Monmouth, New Jersey	1

ORGANIZATION	NO. COPIES
Commander U.S. Naval Ordnance Laboratory ATTN: Technical Library Corona, California	1
Stanford University Stanford Electronics Laboratories ATTN: Dr. J. B. Angell Stanford, California	1
Sylvania Electronic Systems Division of Sylvania Electric Products, Inc. ATTN: Electronic Defense Laboratory P. O. Box 205 Mountain View, California	1
Texas Instruments, Inc. Semiconductor Components Division ATTN: Dr. W. Adcock Dallas, Texas	7
Texas Instruments, Inc. Semiconductor Components Division ATTN: Mr. J. Kilby Dallas, Texas	1
Commander Naval Air Development Center ATTN: Henry Neuberait, Code EL-5A Development Support Division Aeronautical Electronic and Electrical Laboratory Johnsville, Pennsylvania	1
Commanding Officer and Director U.S. Navy Electronics Laboratory Library San Diego 52, California	1
Commander U.S. Naval Underwater Ordnance Station ATTN: Emile(k Jiwad, E.M. Gardiner Newport, Rhode Island	1
Commander Material Laboratory Library Building 291, Code 9123 New York Naval Shipyard Brooklyn 1, New York	1
Armed Services Technical Information Agency ATTN: TIPDR Arlington Hall Station Arlington 12, Virginia	10
Chief, Technical Library Office of Assistant Secretary of Defense (R&D) Room 3E 1065 The Pentagon Washington 25, D.C.	1
Advisory Group on Electron Devices ATTN: M.M. Sorig, Asst. Secretary 346 Broadway, 8th Floor New York 13, New York	2
Advisory Group on Reliability of Electronic Equipment Office, Assistant Secretary of Defense The Pentagon Washington 25, D.C.	1
Secretariat Advisory Group on Electronic Parts ATTN: Brigadier General E.R. Petting, Retired Moore School Building University of Pennsylvania Philadelphia, Pennsylvania	2
National Bureau of Standards Electricity and Electronics Division Engineering Electronics Section ATTN: Mr. Gustave Shapiro Washington 25, D.C.	1
Director National Security Agency ATTN: R.L. Wigington, REMP-2 Fort George G. Meade, Maryland	1
Director National Security Agency ATTN: A.H. Cole, REMP-2 Fort George G. Meade, Maryland	1
Director National Security Agency ATTN: CREF-332, Room 20087, Miss Savakinas Fort George G. Meade, Maryland	1
ITT Laboratories ATTN: Dr. E. B. Johnston 1951 Gleason Street San Fernando, California	1
Arma Division American Dutch Arma Corporation ATTN: Computer Section Garden City, New York	1
Armour Research Foundation Illinois Institute of Technology ATTN: Electrical Engineering Research Mr. V.H. Disney Chicago 16, Illinois	1

Aeronautical Systems Division, AF Avionics Laboratory, Electronic Technology Div, Wright-Patterson AFB, Ohio. Rpt Nr ASD-TDR-63-587. ELECTRON MICROPROBE DEVELOPMENTS FOR INTEGRATED CIRCUIT RESEARCH. Interim report, Oct 62, 24 p., incl illus., tables, 23 refs.

Unclassified Report

Analytic examination of semiconductor surfaces is possible using electron beams with diameters between 100Å to 10,000Å. Previous electron microprobe work in this field is reviewed; promising analytic methods for the future and fundamental limitations in the formation of electron microprobes are discussed. This work, which stresses analysis of semiconductor (or thin film) surfaces, thus complements the reports of Shoulders (1960) and Wells (1961), who stress fabrication of active circuits using electron-beam techniques.

1. Molecular Electronics
2. Integrated Circuits
3. Electron Beams

I. AFSC Project No. 4159, Task No. 415906
II. Contract AF 33(616)-7553
III. Univ. of California, Berkeley, Calif.
IV. T. E. Everhart
V. ERL Series No. 60, Issue No. 461
VI. Not Aval fr OTS
VII. In ASTIA collection

Aeronautical Systems Division, AF Avionics Laboratory, Electronic Technology Div, Wright-Patterson AFB, Ohio. Rpt Nr ASD-TDR-63-587. ELECTRON MICROPROBE DEVELOPMENTS FOR INTEGRATED CIRCUIT RESEARCH. Interim report, Oct 62, 24 p., incl illus., tables, 23 refs.

Unclassified Report

Analytic examination of semiconductor surfaces is possible using electron beams with diameters between 100Å to 10,000Å. Previous electron microprobe work in this field is reviewed; promising analytic methods for the future and fundamental limitations in the formation of electron microprobes are discussed. This work, which stresses analysis of semiconductor (or thin film) surfaces, thus complements the reports of Shoulders (1960) and Wells (1961), who stress fabrication of active circuits using electron-beam techniques.

1. Molecular Electronics
2. Integrated Circuits
3. Electron Beams

I. AFSC Project No. 4159, Task No. 415906
II. Contract AF 33(616)-7553
III. Univ. of California, Berkeley, Calif.
IV. T. E. Everhart
V. ERL Series No. 60, Issue No. 461
VI. Not Aval fr OTS
VII. In ASTIA collection

Aeronautical Systems Division, AF Avionics Laboratory, Electronic Technology Div, Wright-Patterson AFB, Ohio. Rpt Nr ASD-TDR-63-587. ELECTRON MICROPROBE DEVELOPMENTS FOR INTEGRATED CIRCUIT RESEARCH. Interim report, Oct 62, 24 p., incl illus., tables, 23 refs.

Unclassified Report

Analytic examination of semiconductor surfaces is possible using electron beams with diameters between 100Å to 10,000Å. Previous electron microprobe work in this field is reviewed; promising analytic methods for the future and fundamental limitations in the formation of electron microprobes are discussed. This work, which stresses analysis of semiconductor (or thin film) surfaces, thus complements the reports of Shoulders (1960) and Wells (1961), who stress fabrication of active circuits using electron-beam techniques.

1. Molecular Electronics
2. Integrated Circuits
3. Electron Beams

I. AFSC Project No. 4159, Task No. 415906
II. Contract AF 33(616)-7553
III. Univ. of California, Berkeley, Calif.
IV. T. E. Everhart
V. ERL Series No. 60, Issue No. 461
VI. Not Aval fr OTS
VII. In ASTIA collection

Aeronautical Systems Division, AF Avionics Laboratory, Electronic Technology Div, Wright-Patterson AFB, Ohio. Rpt Nr ASD-TDR-63-587. ELECTRON MICROPROBE DEVELOPMENTS FOR INTEGRATED CIRCUIT RESEARCH. Interim report, Oct 62, 24 p., incl illus., tables, 23 refs.

Unclassified Report

Analytic examination of semiconductor surfaces is possible using electron beams with diameters between 100Å to 10,000Å. Previous electron microprobe work in this field is reviewed; promising analytic methods for the future and fundamental limitations in the formation of electron microprobes are discussed. This work, which stresses analysis of semiconductor (or thin film) surfaces, thus complements the reports of Shoulders (1960) and Wells (1961), who stress fabrication of active circuits using electron-beam techniques.

1. Molecular Electronics
2. Integrated Circuits
3. Electron Beams

I. AFSC Project No. 4159, Task No. 415906
II. Contract AF 33(616)-7553
III. Univ. of California, Berkeley, Calif.
IV. T. E. Everhart
V. ERL Series No. 60, Issue No. 461
VI. Not Aval fr OTS
VII. In ASTIA collection

Aeronautical Systems Division, AF Avionics Laboratory, Electronic Technology Div., Wright-Patterson AFB, Ohio. Rpt Nr ASD-TDR-63-587, ELECTRON MICROPROBE DEVELOPMENTS FOR INTEGRATED CIRCUIT RESEARCH Interim report, Oct 62, 24 p., incl illus., tables, 23 refs.

Unclassified Report

Analytic examination of semiconductor surfaces is possible using electron beams with diameters between 100Å to 10,000Å. Previous electron microprobe work in this field is reviewed; promising analytic methods for the future and fundamental limitations in the formation of electron microprobes are discussed. This work, which stresses analysis of semiconductor (or thin film) surfaces, thus complements the reports of Shoulders (1960) and Wells (1961), who stress fabrication of active circuits using electron-beam techniques.

1. Molecular Electronics
2. Integrated Circuits
3. Electron Beams
I. AFSC Project No. 4159 Task No. 415906
II. Contract AF 33(616)-7553
III. Univ. of California Berkeley, Calif.
IV. T. E. Everhart
V. ERL Series No. 60 Issue No. 461
VI. Not Aval fr OTS
VII. In ASTIA collection

Aeronautical Systems Division, AF Avionics Laboratory, Electronic Technology Div., Wright-Patterson AFB, Ohio. Rpt Nr ASD-TDR-63-587, ELECTRON MICROPROBE DEVELOPMENTS FOR INTEGRATED CIRCUIT RESEARCH Interim report, Oct 62, 24 p., incl illus., tables, 23 refs.

Unclassified Report

Analytic examination of semiconductor surfaces is possible using electron beams with diameters between 100Å to 10,000Å. Previous electron microprobe work in this field is reviewed; promising analytic methods for the future and fundamental limitations in the formation of electron microprobes are discussed. This work, which stresses analysis of semiconductor (or thin film) surfaces, thus complements the reports of Shoulders (1960) and Wells (1961), who stress fabrication of active circuits using electron-beam techniques.

1. Molecular Electronics
2. Integrated Circuits
3. Electron Beams
I. AFSC Project No. 4159 Task No. 415906
II. Contract AF 33(616)-7553
III. Univ. of California Berkeley, Calif.
IV. T. E. Everhart
V. ERL Series No. 60 Issue No. 461
VI. Not Aval fr OTS
VII. In ASTIA collection

Aeronautical Systems Division, AF Avionics Laboratory, Electronic Technology Div., Wright-Patterson AFB, Ohio Rpt Nr ASD-TDR-63-587, ELECTRON MICROPROBE DEVELOPMENTS FOR INTEGRATED CIRCUIT RESEARCH Interim report, Oct 62, 24 p., incl illus., tables, 23 refs.

Unclassified Report

Analytic examination of semiconductor surfaces is possible using electron beams with diameters between 100Å to 10,000Å. Previous electron microprobe work in this field is reviewed; promising analytic methods for the future and fundamental limitations in the formation of electron microprobes are discussed. This work, which stresses analysis of semiconductor (or thin film) surfaces, thus complements the reports of Shoulders (1960) and Wells (1961), who stress fabrication of active circuits using electron-beam techniques.

1. Molecular Electronics
2. Integrated Circuits
3. Electron Beams
I. AFSC Project No. 4159 Task No. 415906
II. Contract AF 33(616)-7553
III. Univ. of California Berkeley, Calif.
IV. T. E. Everhart
V. ERL Series No. 60 Issue No. 461
VI. Not Aval fr OTS
VII. In ASTIA collection

Aeronautical Systems Division, AF Avionics Laboratory, Electronic Technology Div., Wright-Patterson AFB, Ohio Rpt Nr ASD-TDR-63-587, ELECTRON MICROPROBE DEVELOPMENTS FOR INTEGRATED CIRCUIT RESEARCH Interim report, Oct 62, 24 p., incl illus., tables, 23 refs.

Unclassified Report

Analytic examination of semiconductor surfaces is possible using electron beams with diameters between 100Å to 10,000Å. Previous electron microprobe work in this field is reviewed; promising analytic methods for the future and fundamental limitations in the formation of electron microprobes are discussed. This work, which stresses analysis of semiconductor (or thin film) surfaces, thus complements the reports of Shoulders (1960) and Wells (1961), who stress fabrication of active circuits using electron-beam techniques.

1. Molecular Electronics
2. Integrated Circuits
3. Electron Beams
I. AFSC Project No. 4159 Task No. 415906
II. Contract AF 33(616)-7553
III. Univ. of California Berkeley, Calif.
IV. T. E. Everhart
V. ERL Series No. 60 Issue No. 461
VI. Not Aval fr OTS
VII. In ASTIA collection

UNCLASSIFIED